Upconversion

International Edition: DOI: 10.1002/anie.201709156
German Edition: DOI: 10.1002/ange.201709156

Controlling Lanthanide Exchange in Triple-Stranded Helicates: A Way to Optimize Molecular Light-Upconversion

Davood Zare, Yan Suffren, Homayoun Nozary, Andreas Hauser, and Claude Piguet**

Abstract: *The kinetic lability of hexadentate gallium-based tripods is sufficient to ensure thermodynamic self-assembly of luminescent heterodimetallic $[GaLn(\mathbf{L3})_3]^{6+}$ helicates on the hour time scale, where Ln is a trivalent 4f-block cation. The inertness is, however, large enough for preserving the triple-helical structure when $[GaLn(\mathbf{L3})_3]^{6+}$ is exposed to lanthanide exchange. The connection of a second gallium-based tripod further slows down the exchange processes to such an extent that spectroscopically active $[CrErCr(\mathbf{L4})_3]^{9+}$ can be diluted into closed-shell $[GaYGa(\mathbf{L4})_3]^{9+}$ matrices without metal scrambling. This feature is exploited for pushing molecular-based energy-transfer upconversion (ETU) at room temperature.*

In his Nobel lecture,[1] Lehn ended the list of his achievements with the introduction of the concept of self-assembly in supramolecular chemistry, which was applied to the preparation of the first planned multinuclear helicate, then referred to as an "inorganic double helix".[2] The apparently miraculous emergence of a highly symmetrical discrete entity from a mixture of sophisticated segmented multidentate ligands and multivalent metal ions was initially thought to be the result of a cooperative driving force having its origin in the favourable matching between the binding possibilities of the ligands and the stereochemical preferences of the metal ions.[3] Subsequent thermodynamic analysis refuted this hypothesis,[4] and kinetic studies established that the ultimate and crucial assembly step leading to inert 3d-block helicates obeyed a keystone mechanism (Scheme 1, left part),[5] whereas more labile 4f-block analogues were obtained by a braiding process (Scheme 1, right part).[6] Only the keystone mechanism is compatible with the instructed and stepwise piling up of different metallic cations along one dimension, an arrangement required for the design of i) directional light-downshifting devices[7] and ii) discrete molecules exhibiting linear light-upconversion.[8]

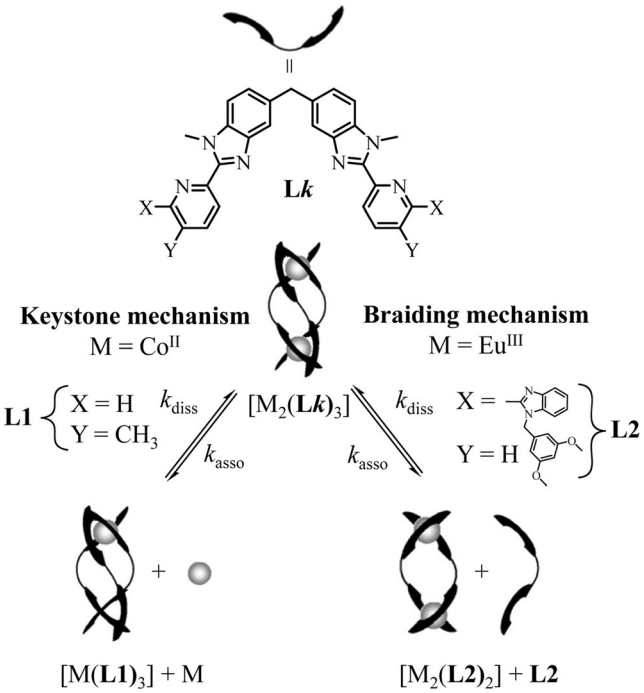

Scheme 1. Ultimate steps of the assembly mechanisms leading to dinuclear d-block (M = Co^{II}, left part)[5a] and f-block (M = Eu^{III}, right part)[6] triple-stranded helicates.

We therefore propose herein to take advantage of the variable kinetic inertness of d-block cations (M^{III}) for mastering the ultimate assembly/disassembly step of dimetallic $[MLn\mathbf{L}_n]$ helicates ($n = 2$–4).[9] An unprecedented keystone mechanism is thus forced to occur even for the labile f-block cations (Ln^{III}).

Inspired by Raymond's report,[11] which claimed that dinuclear Ga^{III}-based triple-stranded helicates possess a remarkable intermediate kinetic regime where racemization occurs without metal-dissociation, we decided to benefit from these favourable characteristics for exploring lanthanide exchange in $[GaY(\mathbf{L3})_3]^{6+}$ [Eq. (1)], a triple-stranded helicate previously fully characterized by ESI-MS, NMR spectroscopy, and X-ray diffraction studies (Scheme 2a).[10]

$$[GaY(\mathbf{L3})_3]^{6+} + Eu^{3+} \underset{k_r}{\overset{k_f}{\rightleftharpoons}} [GaEu(\mathbf{L3})_3]^{6+} + Y^{3+} \quad (1)$$

Upon reaction of $[GaY(\mathbf{L3})_3](CF_3SO_3)_6$ with a stoichiometric amount of $[Eu(CF_3SO_3)_3]$ (written respectively as $[GaY(\mathbf{L3})_3]^{6+}$ and Eu^{3+} for the rest of this work) at millimolar

[*] Dr. D. Zare, Dr. H. Nozary, Prof. Dr. C. Piguet
Department of Inorganic, Analytical and Applied Chemistry
University of Geneva
30 quai E. Ansermet, 1211 Geneva 4 (Switzerland)
E-mail: Claude.Piguet@unige.ch
Dr. Y. Suffren, Prof. Dr. A. Hauser
Department of Physical Chemistry
University of Geneva
30 quai E. Ansermet, 1211 Geneva 4 (Switzerland)
E-mail: Andreas.Hauser@unige.ch
Dr. Y. Suffren
Current address: Institut des Sciences Chimiques de Rennes, INSA, UMR CNRS 6226
35708 Rennes (France)
Supporting information and the ORCID identification number(s) for the author(s) of this article can be found under: https://doi.org/10.1002/anie.201709156.

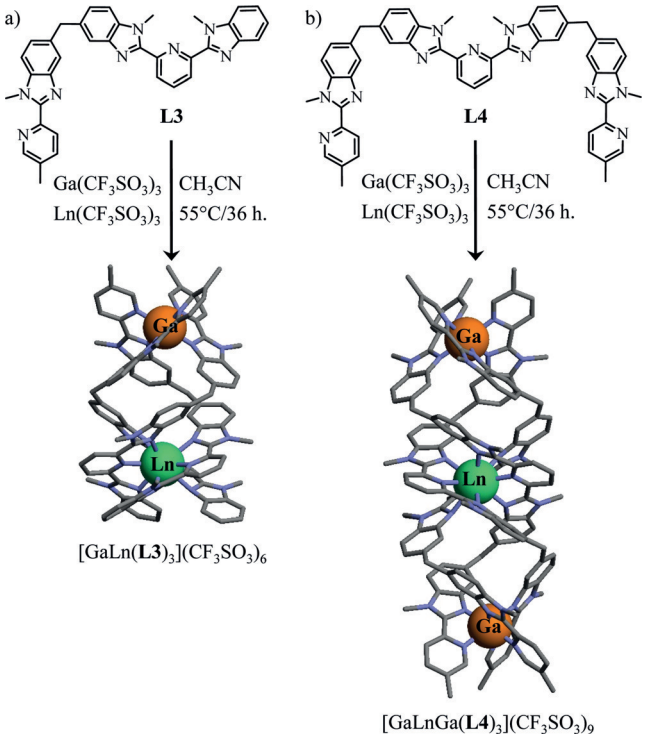

Scheme 2. Self-assembly of a) $[GaLn(\mathbf{L3})_3]^{6+}$ and b) $[GaLnGa(\mathbf{L4})_3]^{9+}$ helicates. The molecular structures correspond to those found in the crystal structures of $[CrEr(\mathbf{L3})_3](CF_3SO_3)_6{\cdot}(C_3H_5N)_{26}$ and $[GaErGa(\mathbf{L4})_3](CF_3SO_3)_9{\cdot}(C_2H_3N)_{35.5}$.[10]

concentrations in acetonitrile, the twenty-two ^{1}H NMR signals of the diamagnetic C_3-symmetrical $[GaY(\mathbf{L3})_3]^{6+}$ helicate (Figure 1a, bottom) are stepwise replaced with those of its paramagnetic $[GaEu(\mathbf{L3})_3]^{6+}$ analogue (Figure 1a, top), this without significant accumulation of any intermediate species. Integration of the NMR signals provided kinetic traces (Figure 1b), the close-to-linear derivative of which (Figure 1c) dismisses the reversible elementary second-order mechanism suggested in Equation (1) (see also Appendix S1 in the Supporting Information).[10]

Consideration of the unsaturated $[Ga(\mathbf{L3})_3]^{3+}$ tripod as a reactive intermediate according to Equation (2) complicates the mechanism and yields the rate equation in Equation (3).

$$[GaY(\mathbf{L3})_3]^{6+} + Eu^{3+} \underset{k_{-1}}{\overset{k_1}{\rightleftharpoons}} [Ga(\mathbf{L3})_3]^{3+} + Y^{3+} + Eu^{3+} \underset{k_{-2}}{\overset{k_2}{\rightleftharpoons}} [GaEu(\mathbf{L3})_3]^{6+} + Y^{3+} \quad (2)$$

$$V = -d|GaY(\mathbf{L3})_3|/dt = k_1|GaY(\mathbf{L3})_3| - k_{-1}|Ga(\mathbf{L3})_3||Y| \quad (3)$$

Applying the steady-state approximation for $[Ga(\mathbf{L3})_3]^{3+}$ [Eq. (4)] followed by its introduction into Equation (3) yields Equation (5) after algebraic transformations.

$$\begin{aligned} &d|Ga(\mathbf{L3})_3|/dt = k_1|GaY(\mathbf{L3})_3| + k_{-2}|GaEu(\mathbf{L3})_3| \\ &\quad -|Ga(\mathbf{L3})_3|(k_{-1}|Y| + k_2|Eu|) = 0 \\ &\Rightarrow |Ga(\mathbf{L3})_3| = (k_1|GaY(\mathbf{L3})_3| + k_{-2}|GaEu(\mathbf{L3})_3|)/(k_{-1}|Y| + k_2|Eu|) \end{aligned} \quad (4)$$

$$V = -\frac{d|GaY(\mathbf{L3})_3|}{dt} = \frac{k_1k_2|GaY(\mathbf{L3})_3||Eu| - k_{-1}k_{-2}|GaEu(\mathbf{L3})_3||Y|}{k_{-1}|Y| + k_2|Eu|} \quad (5)$$

Whereas direct integration of Equation (5) using stoichiometric amounts of initial reactants is not possible (see Appendix S2), the addition of a large excess of free metal ions $|Y| = |Y|^0 \gg |GaY(\mathbf{L3})_3|$ and $|Eu| = |Eu|^0 \gg |GaEu(\mathbf{L3})_3|$ transforms Equation (5) into the simple first-order differential form given in Equation (6), where $|GaY(\mathbf{L3})_3|^0 = |Ga|^{tot}$ and $|GaEu(\mathbf{L3})_3|^0 = 0$ are used as initial conditions (see Appendix S3).

$$\begin{aligned} &-d|GaY(\mathbf{L3})_3|/dt = \alpha|GaY(\mathbf{L3})_3| - \beta \\ &\text{with } \alpha = \frac{k_1k_2|Eu|^0 + k_{-1}k_{-2}|Y|^0}{k_{-1}|Y|^0 + k_2|Eu|^0} \\ &\text{and } \beta = \frac{k_{-1}k_{-2}|Y|^0|GaY(\mathbf{L3})_3|^0}{k_{-1}|Y|^0 + k_2|Eu|^0} \end{aligned} \quad (6)$$

Integration yields an exponential law [Eq. (7)].

$$|GaY(\mathbf{L3})_3| = (|GaY(\mathbf{L3})_3|^0 - \beta/\alpha)e^{-\alpha t} + \beta/\alpha \quad (7)$$

The experimental kinetic traces recorded for the reaction of $[GaY(\mathbf{L3})_3]^{6+}$ with Eu^{3+} in presence of different fixed excess concentrations of Y^{3+} and Eu^{3+} indeed provided decay traces (blue diamonds in Figure 2 and Figure S1), which could be conveniently fitted to Equation (7) (red traces in Figure 2 and Figure S1) The α and β values obtained at different excess concentrations are collected in Table S1 (Supporting Information). Subsequent non-linear least-square fitting of α and β according to Equation (6) gave the set of rate constants $k_1 = 0.1(2)\ s^{-1}$, $k_2 = 480(81)\ M^{-1}s^{-1}$, $k_{-1} = 240(41)\ M^{-1}s^{-1}$ and $k_{-2} = 0.1(1)\ s^{-1}$ (CD_3CN, 293 K, Table 1), from which satisfying kinetic traces can be rebuilt (green triangles in Figure 2 and Figure S1).

Comparing the dissociative rate constants k_{diss} gathered for 3d-block helicates (entries 4–5 in Table 1) with those found for the related processes operating around 4f-block cations (entries 1–3 in Table 1) highlights an increase in lability by 3–4 orders of magnitude when Co^{2+} or Fe^{2+} are replaced with Y^{3+} and Eu^{3+}. The latter kinetic discrimination logically provides self-assembled heterodinuclear $[GaY(\mathbf{L3})_3]^{6+}$ and $[GaEu(\mathbf{L3})_3]^{6+}$ helicates, which can be sequentially disentangled. The lanthanide cations can be indeed selectively released from these complexes according to an unprecedented keystone mechanism, while the d-block cation keeps the triple-helical structure intact. Interestingly, the unthreading process required for the dissociation of one Eu^{III} cation from the double-stranded helicate $[Eu_2(\mathbf{L2})_2]^{6+}$ ($k_{diss} = 0.17(1)\ s^{-1}$, entry 3 in Table 1) is as efficient as that found in the triple-stranded helicate $[GaEu(\mathbf{L3})_3]^{6+}$ ($k_{diss} = 0.1(1)\ s^{-1}$, entry 1 in Table 1), but the reverse complexation process requires much more reorganization around the triple-stranded $[Ga(\mathbf{L3})_3]^{3+}$ precursor ($k_{asso} = 480(81)\ M^{-1}s^{-1}$) than around a double-stranded $[Eu(\mathbf{L2})_2]^{3+}$ scaffold ($k_{asso} = 2.2(4) \times 10^6\ M^{-1}s^{-1}$). The thermodynamic constants estimated for the formation of $[GaLn(\mathbf{L3})_2]^{6+}$ helicates display the expected trend $\beta_{1,1}^{Ga(\mathbf{L3})_3,Eu} > \beta_{1,1}^{Ga(\mathbf{L3})_3,Y}$, which is diagnostic for the hin-

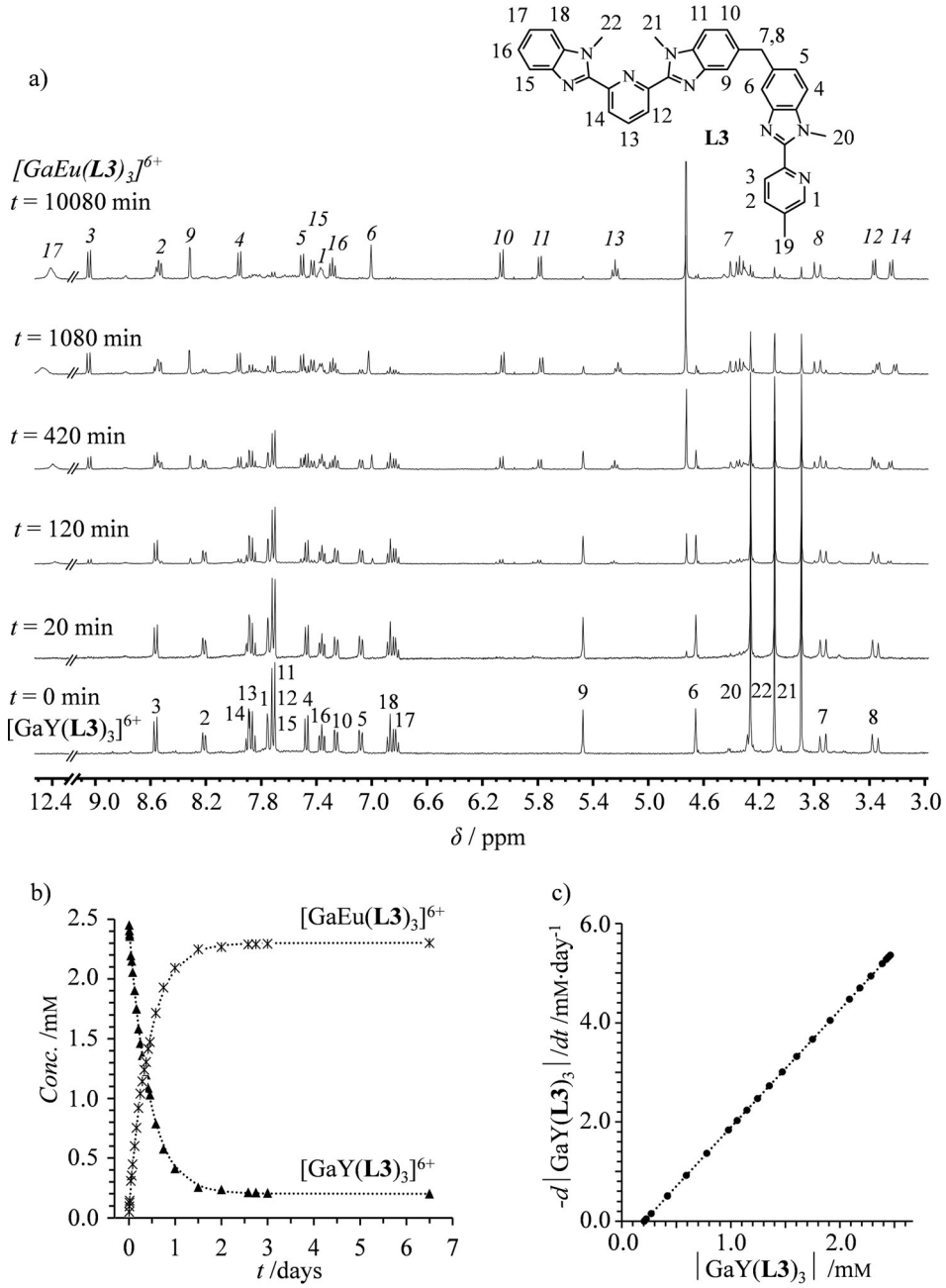

Figure 1. a) Reaction of $[GaY(\mathbf{L3})_3](CF_3SO_3)_6$ (1.0 equiv., $c = 2.5$ mM) with $Eu(CF_3SO_3)_3$ (1.0 equiv.) monitored by ^1H NMR spectroscopy measured in CD_3CN at 293 K for 7 days. The numbering scheme is shown. b) Associated kinetic traces (the dotted traces correspond to the best fits according to Equation (2)) and c) time-derivative of the kinetic trace (the dotted line shows a linear fit). Adapted from Ref. [10].

dered tight wrapping of tridentate 2,6-bis(benzimidazol-2-yl)pyridine binding units around smaller trivalent lanthanides.[12] The latter hampered threading process is also responsible for the reduction of $\beta_{1,1}^{Ga(\mathbf{L3})_3,Ln}$ by 2 orders of magnitude when compared to related stability constants obtained for chromium–lanthanide helicates $[CrLn(\mathbf{L6})_3]^{6+}$ ($10^{5.3} \leq \beta_{1,1}^{Cr(\mathbf{L6})_3,Ln} \leq 10^{5.9}$),[13] in which **L6** is identical to **L3** except for the replacement of the terminal N-donor benzimidazole units with less bulky *N*,*N*′-diethylcarboxamide O-donor groups (Scheme S1 in the Supporting Information). Kinetic inertness can be further improved by the connection of a second Ga^{III}-based tripod in the trinuclear dimetallic helicates $[GaLnGa(\mathbf{L4})_3]^{9+}$, the structure of which was previously established by X-ray diffraction, ESI-MS and NMR spectroscopy (Scheme 2b).[10] Mixing $[GaYGa(\mathbf{L4})_3]^{9+}$ with Eu^{3+} in acetonitrile leads to no change over periods of months (Figure S2), an inertness which was exploited for preparing solid-state solutions of closed-shell $[GaYGa(\mathbf{L4})_3](CF_3SO_3)_9$, in which variable amounts (2%, 10%) of isostructural inert, but optically active $[CrErCr(\mathbf{L4})_3](CF_3SO_3)_9$ were dispersed by co-crystallization.[8b]

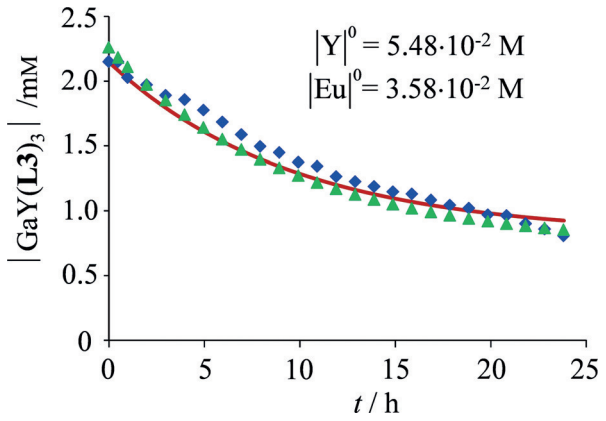

Figure 2. Experimental (blue diamonds) and fitted [Eq. (7), red trace with α and β taken from Table S1) time-dependent concentrations of $[GaY(\mathbf{L3})_3]^{6+}$ according to Equation (2) ($|GaY(\mathbf{L3})_3|^0 = 2.15\times10^{-3}$ M, $|GaEu(\mathbf{L3})_3|^0 = 0$ M, CD_3CN, 293 K). The green triangles correspond to the rebuilt kinetic trace using the final set of rate constants $k_1 = 0.1$-(2) s^{-1}, $k_2 = 480(81)$ $M^{-1}s^{-1}$, $k_{-1} = 240(41)$ $M^{-1}s^{-1}$, $k_{-2} = 0.1(1)$ s^{-1}.

Table 1: Rate constants and thermodynamic formation constants ($\beta_{1,1}^{ML_n,M'}$)[a] determined for the keystone mechanism operating in multiple-stranded helicates.

Entry	Rate constants	$\beta_{1,1}^{ML_n,M'}/M^{-1}$[a]	Conditions	Ref.
1	$[Ga(\mathbf{L3})_3]^{3+} + Eu^{3+} \underset{k_{diss}=0.1(1)\,s^{-1}}{\overset{k_{asso}=480(81)\,M^{-1}s^{-1}}{\rightleftharpoons}} [GaEu(\mathbf{L3})_3]^{6+}$	$10^{3.7(1)}$	CH_3CN 293 K	This work
2	$[Ga(\mathbf{L3})_3]^{3+} + Y^{3+} \underset{k_{diss}=0.1(2)\,s^{-1}}{\overset{k_{asso}=240(41)\,M^{-1}s^{-1}}{\rightleftharpoons}} [GaY(\mathbf{L3})_3]^{6+}$	$10^{3.4(1)}$	CH_3CN 293 K	This work
3	$[Eu(\mathbf{L2})_2]^{3+} + Eu^{3+} \underset{k_{diss}=0.17(1)\,s^{-1}}{\overset{k_{asso}=2.2(4)\times10^6\,M^{-1}s^{-1}}{\rightleftharpoons}} [Eu_2(\mathbf{L2})_2]^{6+}$	$10^{7.11(7)}$	CH_3CN 298 K	[6a]
4	$[Co(\mathbf{L1})_3]^{2+} + Co^{2+} \underset{k_{diss}=1.4(2)\times10^{-5}\,s^{-1}}{\rightleftharpoons} [Co_2(\mathbf{L1})_3]^{4+}$[b]	–	CH_3CN 293 K	[5a]
5	$[Fe(\mathbf{L5})_3]^{2+} + Fe^{2+} \underset{k_{diss}=7(2)\times10^{-5}\,s^{-1}}{\overset{k_{asso}=1.1(3)\times10^{-3}\,M^{-1}s^{-1}}{\rightleftharpoons}} [Fe_2(\mathbf{L5})_3]^{4+}$[c]	$10^{1.2(1)}$	CH_3OH 298 K	[5b]

[a] The thermodynamic constants are deduced from the ratio of the rate constants $\beta_{1,1}^{ML_n,M'} = k_{asso}/k_{diss}$ and expressed in M^{-1}. Fixing the standard concentration of the reference state to $c^\theta = 1$ M restores thermodynamic equilibrium constants with no units. [b] k_{diss} is taken as the rate constant of racemization of $[Co_2(\mathbf{L1})_3]^{4+}$.[5a] [c] **L5** is a bis(2,2′-bipyridine) ligand (Scheme S1).[5b]

Upon near-Infrared (NIR) excitation of the spin-flip $Cr(^2T_1,^2E \leftarrow {}^4A_2)$ transitions in the molecular complex $[CrErCr(\mathbf{L4})_3]^{9+}$ ($700 \le \lambda_{exc} \le 750$ nm), the energy-transfer upconversion (ETU) green $Er(^4S_{3/2} \rightarrow {}^4I_{15/2})$ emission, originally detected in frozen acetonitrile[8a] and in pure solid samples at low temperature,[8b] is found to be magnified by one order of magnitude in 10% solid-state solutions (red dots in Figures 3a and Figures S3,S4). This trend is assigned to the concomitant benefits produced by i) the larger concentration of the upconverting $[CrErCr(\mathbf{L4})_3]^{9+}$ devices (mole fraction = 0.10) compared to that found in the acetonitrile/propionitrile solution (mole fraction $= 5.5\times10^{-4}$) and ii) the decrease of luminescence self-quenching and cross-relaxation deactivation pathways in diluted solutions with respect to pure solid samples. The detection of upconverted signals at room temperature for Er-centred molecular-based linear ETU is sufficiently rare to be highlighted herein (Figure 3c and Figure S5).[14] Submitted to the same dilution procedure, the roughly ten-times weaker upconverted signal observed for the dinuclear $[CrEr(\mathbf{L3})_3]^{6+}$ helicate[8b] disappeared when 2–10% of the complex were co-crystallized with the isostructural closed-shell $[GaY(\mathbf{L3})_3](CF_3SO_3)_6$ matrix (Figure 3b, blue triangles). In line with our kinetic data, the several days period required for the crystallization of doped solid-state solutions is accompanied by metal scrambling and the formation of competitive and upconverting-inactive $[GaEr(\mathbf{L3})_3]^{6+}$ and $[CrY(\mathbf{L3})_3]^{6+}$ species. The concentration of molecular $[CrEr(\mathbf{L3})_3]^{6+}$ complex is reduced to such an extent that the intensity of the upconverted signal is lost and the upconversion process cannot take advantage of any dilution process.

In conclusion, we showed that the trigonal $[Ga^{III}N_6]$ non-covalent tripod has an intermediate kinetic regime, which is well adapted for the selective complexation of labile trivalent lanthanides, Ln^{III}, to give triple-stranded $[GaLn(\mathbf{L3})_3]^{6+}$ helicates. The kinetic analysis suggests the operation of a keystone mechanism during which the fixation of labile Ln^{III} to $[Ga(\mathbf{L3})_3]^{3+}$ as well as its release from $[GaLn(\mathbf{L3})_3]^{6+}$ require considerable reorganization of the strands. The reorganization process can be further slowed down by the attachment of a second $[Ga^{III}N_6]$ non-covalent tripod in trinuclear $[GaLnGa(\mathbf{L4})_3]^{9+}$. The kinetics of lanthanide exchange then becomes so slow that closed-shell $[GaYGa(\mathbf{L4})_3](CF_3SO_3)_9$ can serve as a spectroscopically inactive matrix for the dilution of the isostructural open-shell $[CrErCr(\mathbf{L4})_3](CF_3SO_3)_9$ helicate without detectable metal scrambling, thus leading to the detection of molecular upconversion at room temperature. This kinetic control opens avenues for optimizing molecular-based NIR-to-visible upconversion operating in processable materials at room temperature.

Experimental Section

The complexes $[MLn(\mathbf{L3})_3](CF_3SO_3)_6$ and $[MLnM(\mathbf{L4})_3](CF_3SO_3)_9$ were prepared according to literature procedures (M = Cr, Ga and Ln = Er, Y.[10] The trifluoromethanesulfonate salts $Ln(CF_3SO_3)_3$ (Ln = Eu, Y) were prepared from the corresponding oxides (Aldrich 99.99%).[15] Diluted solid-state samples were obtained by slow diffusion of tert-butylmethylether into concentrated acetonitrile solutions containing 2–10% mole fraction of $[CrErCr(\mathbf{L4})_3](CF_3SO_3)_9$ in 98–90% of $[GaYGa(\mathbf{L4})_3](CF_3SO_3)_9$. ^1H NMR spectra were recorded at 293 K on a Bruker Avance 400 MHz spectrometer from CD_3CN solutions. Chemical shifts are given in ppm with respect to tetramethylsilane $Si(CH_3)_4$. The detailed experimental setup and procedure for recording light-upconverted spectra have been reported previously.[8,10] The mathematical analyses were performed by using Igor Pro (WaveMetrics Inc.) and Excel (Microsoft) software.

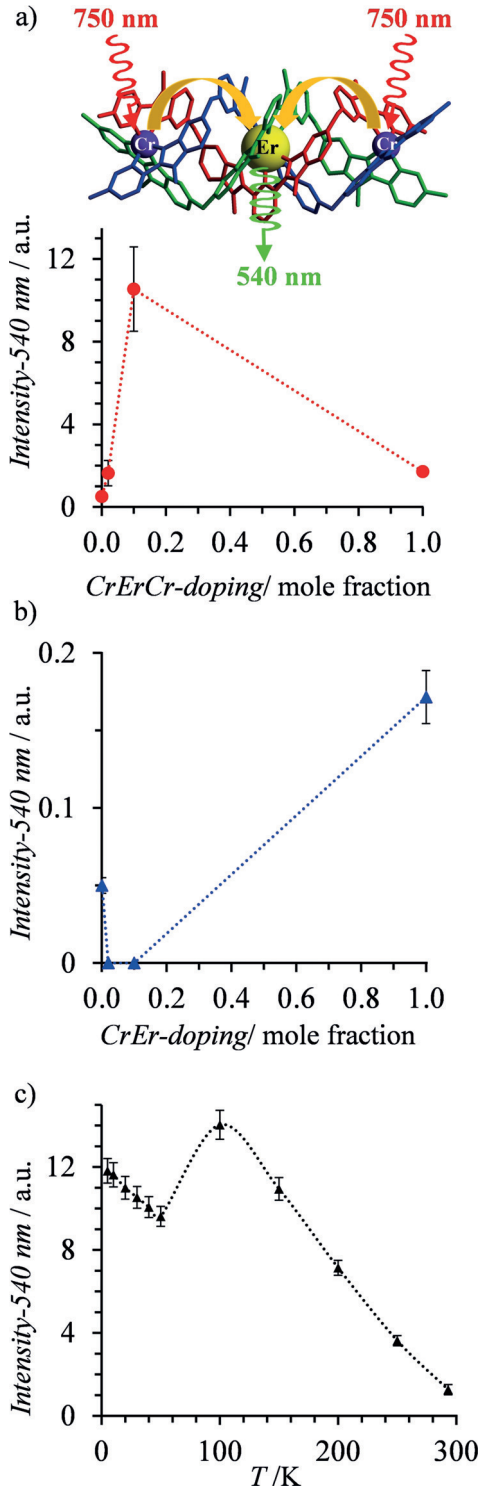

Figure 3. Intensity of green (540 nm) Er($^4S_{3/2}\rightarrow{}^4I_{15/2}$) ETU emission in a) $[CrErCr(\mathbf{L4})_3](CF_3SO_3)_9$ (red dots) as a function of its doping level into isostructural $[GaYGa(\mathbf{L4})_3](CF_3SO_3)_9$ matrix at 31 K and b) $[CrEr(\mathbf{L3})_3](CF_3SO_3)_6$ (blue triangles) as a function of its doping level in isostructural $[GaY(\mathbf{L3})_3](CF_3SO_3)_6$ matrix at 31 K. c) Intensity of green (540 nm) Er($^4S_{3/2}\rightarrow{}^4I_{15/2}$) ETU emission observed for 10% $[CrErCr(\mathbf{L4})_3](CF_3SO_3)_9$ doped into $[GaYGa(\mathbf{L4})_3](CF_3SO_3)_9$ as a function of temperature ($\lambda_{exc}=750\pm5$ nm, incident power = 125 mW, the excitation beam was loosely focused on the sample with a 100 mm lens). The dotted traces are only guides for the eyes.

Acknowledgements

This work is supported through grants from the Swiss National Science Foundation.

Conflict of interest

The authors declare no conflict of interest.

Keywords: helicates · heterometallic complexes · keystone mechanism · kinetics · molecular upconversion

How to cite: *Angew. Chem. Int. Ed.* **2017**, *56*, 14612–14617
Angew. Chem. **2017**, *129*, 14804–14809

[1] J.-M. Lehn, *Angew. Chem. Int. Ed. Engl.* **1988**, *27*, 89–112; *Angew. Chem.* **1988**, *100*, 91–116.

[2] J.-M. Lehn, A. Rigault, J. Siegel, J. Harrowfield, B. Chevrier, D. Moras, *Proc. Natl. Acad. Sci. USA* **1987**, *84*, 2565–2569.

[3] a) T. M. Garrett, U. Koert, J.-M. Lehn, *J. Phys. Org. Chem.* **1992**, *5*, 529–532; b) A. Pfeil, J.-M. Lehn, *J. Chem. Soc. Chem. Commun.* **1992**, 838–839; c) A. F. Williams, C. Piguet, R. Carina, *Transit. Met. Supramolecular Chem.* **1994**, *448*, 409–424; d) J.-M. Lehn, A. V. Eliseev, *Science* **2001**, *291*, 2331–2333.

[4] a) G. Ercolani, *J. Am. Chem. Soc.* **2003**, *125*, 16097–16103; b) J. Hamacek, C. Piguet, *J. Phys. Chem. B* **2006**, *110*, 7783–7792.

[5] a) L. J. Charbonnière, A. F. Williams, U. Frey, A. E. Merbach, P. Kamalaprija, O. Schaad, *J. Am. Chem. Soc.* **1997**, *119*, 2488–2496; b) N. Fatin-Rouge, S. Blanc, E. Leize, A. van Dorsselaer, P. Baret, J.-L. Pierre, A. M. Albrecht-Gary, *Inorg. Chem.* **2000**, *39*, 5771–5778; c) N. Fatin-Rouge, S. Blanc, A. Pfeil, A. Rigault, A.-M. Albrecht-Gary, J.-M. Lehn, *Helv. Chim. Acta* **2001**, *84*, 1694–1711.

[6] a) J. Hamacek, S. Blanc, M. Elhabiri, E. Leize, A. van Dorsselaer, C. Piguet, A. M. Albrecht-Gary, *J. Am. Chem. Soc.* **2003**, *125*, 1541–1550; b) M. Elhabiri, J. Hamacek, J.-C. G. Bünzli, A. M. Albrecht-Gary, *Eur. J. Inorg. Chem.* **2004**, 51–62.

[7] a) S. Torelli, S. Delahaye, A. Hauser, G. Bernardinelli, C. Piguet, *Chem. Eur. J.* **2004**, *10*, 3503–3516; b) L. Aboshyan-Sorgho, H. Nozary, A. Aebischer, J.-C. G. Bünzli, P.-Y. Morgantini, K. R. Kittilstved, A. Hauser, S. V. Eliseeva, S. Petoud, C. Piguet, *J. Am. Chem. Soc.* **2012**, *134*, 12675–12684.

[8] a) L. Aboshyan-Sorgho, C. Besnard, P. Pattison, K. R. Kittilstved, A. Aebischer, J.-C. G. Bünzli, A. Hauser, C. Piguet, *Angew. Chem. Int. Ed.* **2011**, *50*, 4108–4112; *Angew. Chem.* **2011**, *123*, 4194–4198; b) Y. Suffren, D. Zare, S. V. Eliseeva, L. Guénée, H. Nozary, T. Lathion, L. Aboshyan-Sorgho, S. Petoud, A. Hauser, C. Piguet, *J. Phys. Chem. C* **2013**, *117*, 26957–26963.

[9] a) S. Rigault, C. Piguet, G. Bernardinelli, G. Hopfgartner, *Angew. Chem. Int. Ed.* **1998**, *37*, 169–172; *Angew. Chem.* **1998**, *110*, 178–181; b) M. Cantuel, G. Bernardinelli, D. Imbert, J.-C. G. Bünzli, G. Hopfgartner, C. Piguet, *J. Chem. Soc. Dalton Trans.* **2002**, 1929–1940.

[10] D. Zare, Y. Suffren, L. Guénée, S. V. Eliseeva, H. Nozary, L. Aboshyan-Sorgho, S. Petoud, A. Hauser, C. Piguet, *Dalton Trans.* **2015**, *44*, 2529–2540.

[11] a) B. Kersting, M. Meyer, R. E. Powers, K. N. Raymond, *J. Am. Chem. Soc.* **1996**, *118*, 7221–7222; b) M. Meyer, B. Kersting, R. E. Powers, K. N. Raymond, *Inorg. Chem.* **1997**, *36*, 5179–5191.

[12] S. Petoud, J.-C. G. Bünzli, F. Renaud, C. Piguet, K. J. Schenk, G. Hopfgartner, *Inorg. Chem.* **1997**, *36*, 5750–5760.

[13] M. Cantuel, G. Bernardinelli, G. Muller, J. P. Riehl, C. Piguet, *Inorg. Chem.* **2004**, *43*, 1840 – 1849.
[14] A. Nonat, C. F. Chan, C. Platas-Iglesias, Z. Liu, W.-T. Wong, W.-K. Wong, K.-L. Wong, L. J. Charbonnière, *Nat. Commun.* **2016**, *11978*, 1 – 8.
[15] J. F. Desreux, *Lanthanide Probes in Life, Chemical and Earth Sciences* (Eds.: G. Choppin, J.-C. G. Bünzli), Elsevier, Amsterdam, **1989**, chapter 2.

Manuscript received: September 5, 2017
Accepted manuscript online: September 28, 2017
Version of record online: October 16, 2017

